Surface phonons of Na-induced superstructures on Al(111)

T. Nagao,* Y. Iizuka, T. Shimazaki, and C. Oshima
Department of Applied Physics, Waseda University, 3-4-1 Okubo Shinjuku, Tokyo, Japan
(Received 21 June 1996)

We report the surface phonon measurement by high-resolution electron-energy-loss spectroscopy of the Na-induced superstructures on Al(111). Semiempirical simple lattice dynamical analysis using several central forces is applied to understand qualitatively the vibrational properties of the system as a first step. The lattice dynamical calculation for the Al(111)-$(\sqrt{3}\times\sqrt{3})R30°$-Na surface with a substitutional adsorption geometry reproduces the observed strongly dispersing surface resonant mode, while the calculated dispersion curves for a threefold adsorption geometry differ largely from the observed ones. This is explained in terms of the structural difference which causes different restoring forces at Na atoms. The observed dipole active surface resonant mode at the $\bar{\Gamma}$ point is assigned to a perpendicular motion of Na against the almost fixed substrate which is similar to the one of which frequency was determined by some *ab initio* calculations. For the Al(111)-(2×2)-Na surface, the measured surface phonon dispersion curves locate very close to Rayleigh mode of the clean Al(111) and its backfold at $\bar{M}'$ point. [S0163-1829(97)07416-X]

I. INTRODUCTION

The adsorption of atoms on crystal surfaces constitutes a wide area of study which still uncovers fundamental questions. Recently, the study of alkali-metal adsorption has attracted much attention in experimental as well as theoretical research.[1–7] Much of the interest has centered on the electronic structure, and phenomena related hereto, such as characteristic coverage dependence of the work function, dynamic dipole, and phonon frequency. From the standpoint of structure analysis, recent studies have revealed that some of the alkali-metal adsorbed crystal systems show thorough reconstruction of the substrate which sometimes involves the intermixing (alloying) of adsorbed atoms and substrate atoms.[8–11] These structural results have cast a doubt upon the widely accepted assumption of high symmetry adsorption sites on the unreconstructed substrate surfaces, and added another dimension to the discussion of the nature of alkali-metal adsorption. For alkali-metal adsorbed Al(111), which was widely believed to take a simple adsorption site of high symmetry sites on unreconstructed substrate, recent surface extended x-ray-absorption fine structure (SEXAFS),[12] and low-energy electron-diffraction[13] (LEED) studies have concluded the substitutional adsorption geometry. These results are also consistent with the results of normal-incidence x-ray standing-wave,[14] high-resolution electron-energy-loss-spectroscopy (HREELS),[15] high-resolution core-level spectroscopy,[16] and *ab initio* total energy calculations based on density-functional theory.[17]

From the standpoint of the vibrational properties, several theoretical and experimental studies were done for alkali-metal adsorbed systems. A theoretical calculation for jellium surfaces predicted the lowering in the vibrational frequency with the increase of coverage.[18] This was explained in terms of the electron redistribution around the adatom due to the orbital hybridization between alkali-metal atoms. By the use of HREELS, a decrease in the dynamic dipole with coverage was reported for alkali-metal adsorbed Cu(111), Cu(100), Cu(110) surfaces.[19,20] In contrast to the dramatic change in both the static and dynamic dipole, energy positions of alkali-induced loss peaks change little with the coverage. However, their vibrational energies correspond fairly well to that predicted by the jellium theory. For the Na adsorbed Al(111) surface, which is one of the most popular systems for *ab initio* calculations, the measured vibrational frequency has been found to correspond very well to the recently calculated one by *ab initio* pseudopotential theory.[15] The observed frequency for Na and Li adsorbed systems did not show any coverage dependence within the precision of 0.3 meV while the work function and dynamic dipole change largely. This was explained in terms of the strong screening of the adsorbate-adsorbate interaction in the substitutional adsorption geometry. The vibrational frequencies change little since the electron density forming the substrate-adsorbate bonding is well screened by the electrons of substrate Al atoms. On the contrary, the work function (static dipole) and the loss intensity (dynamic dipole) change largely due to the charge redistribution in the region above the adatoms where the screening by the substrate electron is absent.

The purpose of the present paper is to investigate first the phonon dispersions of the metal-induced superstructures on a crystal surface. The surface phonon dispersion measurement for a gas adsorbed system provides a good deal of information of substrate-molecule and intramolecule bonding, and its adsorption geometry, together with that of the substrate atomic arrangement. The measurement of a metal-adsorbed system is also expected to provide such a variety of noble information. However, curiously enough, a study from the viewpoint of lattice dynamics has been lacking so far. In this sense, to add new insight and understanding of the metal-adsorbed crystal system, we report the phonon dispersion measurement for Na adsorbed Al(111), which in a theoretical sense, is the most prototypical system among metal-adsorbed metal systems. Since the Na-induced superstructure on Al(111) takes a peculiar structure of substitutional adsorption geometry (which, in a sense, can be called surface alloy) the system is also expected to provide attractive vibrational in-

formation from the side of structure analysis as well as from the side of electronic properties which has been recently discussed in some *ab initio* calculations.

II. EXPERIMENT

The experiments were carried out in a two-stage ultrahigh vacuum chamber with the base pressure maintained in the 10^{-9} Pa range. In the upper stage, a rear-view type of LEED optics and the cylindrical deflector analyzer for Auger electron spectroscopy (AES) are equipped. The lower stage contains a tandem type of HREEL spectrometer which is shielded triply by permalloy tubes to reduce the magnetic field below 1 mGauss. The energy resolution of the HREEL spectrometer in the straight through mode was 1.2 meV [full width at half maximum (FWHM)] and the typical energy-width of the electron beam that scattered from the Al(111) sample was 2 meV (FWHM).[21] Work function changes were also measured to a precision of ± 2.5 meV by retarding potential method using the monochromatic electron beam in the HREELS instrument.

The Al(111) sample (12 mm diameter, 2 mm thick) was cut by the spark erosion method and polished mechanically to a high optical finish with alumina powder. The surface was cleaned in the UHV chamber by repeated cycles of 4 KV Ar ion bombardment and following annealing up to 600 K. After this cleaning procedure, the AES signals of C and O were well below 1% of the Al signal and the sharp LEED pattern was observed. Alkali metals were deposited onto the clean surface from a thoroughly outgassed SAES getter source. The coverage of the alkali metal was monitored by LEED, AES, and work function measurements.

III. RESULTS AND DISCUSSIONS

In this section, first we show the phonon dispersion curves of the clean Al(111) surface, and then we present the dispersion curves of the Na adsorbed Al(111) surfaces. Lattice dynamical calculations for bulk Al and Al(111) are briefly mentioned, and afterwards, the analysis for Al(111)-$(\sqrt{3}\times\sqrt{3})R30°$-Na is discussed. Finally, the phonon dispersions of Na-adsorbed Al(111)-(2×2) are presented.

A. Surface phonons of the clean Al(111) surface

The lattice dynamical analysis in the present work is based on the central force model the interatomic force constants of which are determined phenomenologically via fittng to the experimental dispersion curves. Bulk force constants (BFC's) in the present calculations were determined by fitting to the phonon dispersion curves of the bulk Al measured by inelastic neutron scattering. Figure 1 shows the measured bulk phonon dispersion curves by Stedman and Nilsson[22] (filled circles) and the calculated phonon dispersion curves in this work (solid curves). Lock *et al.* succeeded in reproducing very precisely the measured bulk phonons by introducing 23 FC's for up to ten nearest neighbors (10 NN).[23] In the present work, on the contrary, only essential 4 BFC's up to 2NN were used. The simple model with a small number of FC's will possibly degrade the fit to the experimental data and may lead to an erroneous conclusion concerning the polarization of the vibrational modes. However, since the goal of this work is to understand the vibrational property of the system qualitatively as a first step, we start with employing a simpler scheme by reducing the number of FC's. In the calculation, two stretching and two tangential FC's up to 2NN bonds are introduced. The reproduced dispersion curves show some deviation from the measured ones. However, an overall fit to the measured dispersion curves is reasonably good in spite of the simplicity in the model. The unique solution of BFC's determined in the present model is listed in the left hand side of Table I. The values are deviating from those reported in the previous work, for example, the 1NN stretching FC α_1 differs 15% compared to that reported in Ref. 23 since the effect of the further 19 parameters are missing.

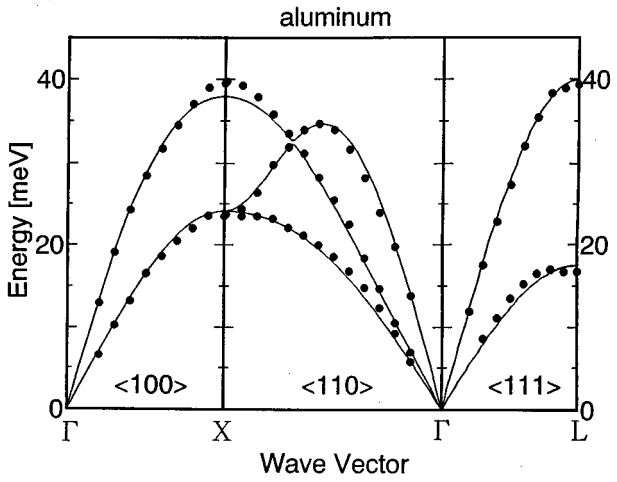

FIG. 1. The solid lines denote the calculated bulk phonon dispersions of Al by a force constant model. In spite of the small number of the fitting parameters used in this calculation (two stretching and two tangential SFC's up to 2NN bonds), the overall agreement between the calculated dispersion curves and the measured ones by inelastic neutron scattering (filled circles) is reasonably good.

Prior to the measurement of the Na adsorbed Al(111) surfaces, the clean Al(111) surface has been measured. Figure 2 shows typical angle-resolved HREEL spectra of the clean Al(111) surface taken with 35.3 eV primary energy. Gain and loss peaks of Rayleigh phonon appear clearly in each spectra. It is clearly visible that the peak positions shift as the incident angle of the electron beam changes. In Fig. 3 we show the dispersion curves along the $\overline{\Gamma M}$ symmetry of the

TABLE I. The uniquely determined FC's values of bulk Al obtained by fitting to the neutron inelastic scattering data (left hand side). A solution of the SFC's obtained by fitting to the Rayleigh mode measured by AR-HREELS for the Al(111) surface (right hand side).

Bulk force constant (BFC) (N/m)	Surface force constant (SFC) (N/m)
$\alpha_1=20400$	$\alpha_{1s}=20400$
$\beta_1=-1800$	$\beta_{1s}=0$
$\alpha_2=3000$	$\alpha_{2s}=3000$
$\beta_2=-400$	$\beta_{2s}=0$

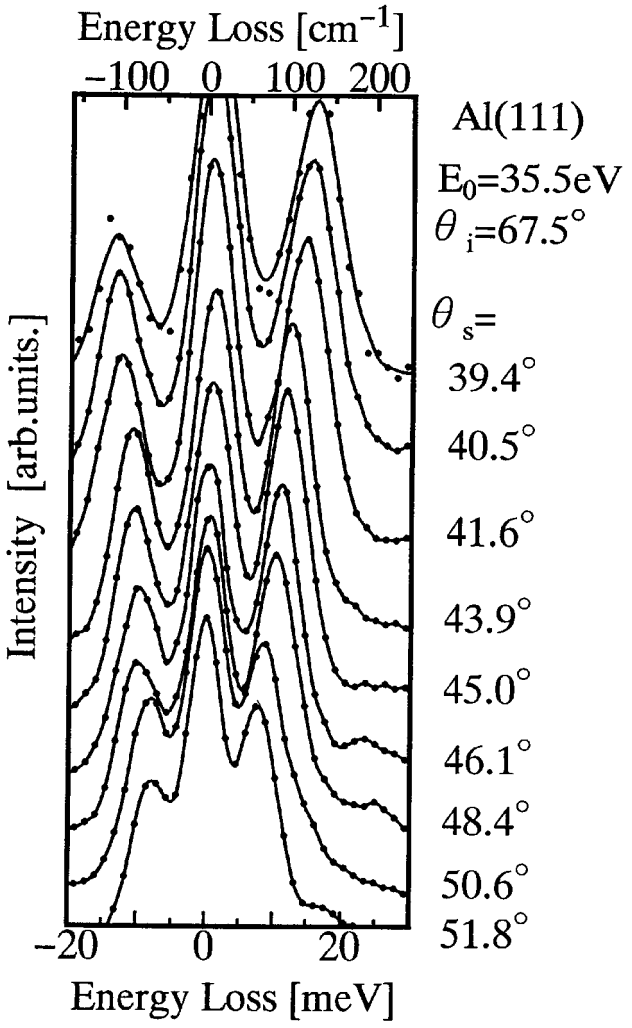

FIG. 2. Typical angle-resolved HREEL spectra of the clean Al(111) surface taken at 35.5 eV primary energy. Gain and loss peaks of the Rayleigh phonon are clearly visible.

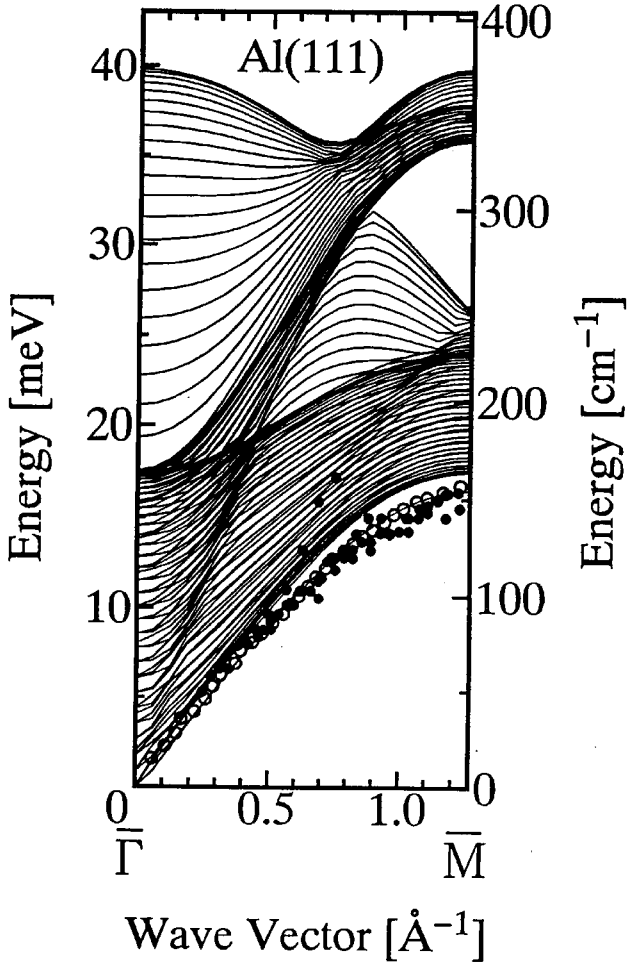

FIG. 3. Observed Rayleigh mode of Al(111) measured by HREELS (filled circles) and He atom scattering (white ones). The observed dispersion curves measured by the two different techniques were found to correspond well. Solid curves show calculated phonon dispersion curves for a 31-atomic-layer slab terminated with (111) faces using four BFC's and two SFC's.

two dimensional Brillouin zone. The data points, taken at several primary energies (4, 12, 16.5, 35.5, 36.7 eV) are indicated by the filled circles. When we compare the present data with the preceding results of He atom scattering by Lock *et al.* (indicated by open circles),[23,24] good agreement is found for the measured Rayleigh mode except for slightly lower energy around M point. In this measurement, clear evidence of the longitudinal surface phonon was not recognized except for the blurred background above 20 meV.

Solid curves in Fig. 3 are the results of the calculated dispersion curves using a slab method. Here, the fitting was done for the observed Rayleigh mode using stretching 1NN and 2NN SFC's of the bonds between the first and the second layer. This preliminary calculation fits well to the measured one, and its vibrational amplitude is strongly localized at the surface top layer at M point, which is the characteristics of Rayleigh mode. However, compared to the preceding works,[24] the present model is much simpler and should be tested, for example, by seeing other surface modes. In fact, the longitudinal surface phonon—which is not yet experimentally detected but reported in a first-principles calculation[25]—is not reproduced in this calculation. The determined SFC's values are listed in the right hand side of Table I.

B. Surface phonons of Na-adsorbed Al(111)-$(\sqrt{3}\times\sqrt{3})R30°$

The alkali induced reconstruction of the Al(111) surface was recently studied by several groups. Surface extended x-ray-adsorption fine structure data[12] and *ab initio* density-functional calculations[17] showed that Na atoms displace Al atoms at 300 K and occupy sixfold coordinated holes in a $(\sqrt{3}\times\sqrt{3})R30°$ geometry (see Fig. 4). A recent study of a LEED intensity analysis also concluded the substitutional adsorption geometry.[13] From the standpoint of atomic vibrations, two *ab initio* calculations have been done for the same Al(111)-Na system and have derived the vibrational frequencies of a mode in which Na atoms move perpendicular to a frozen substrate.[17,18] The validity of the assumption of this polarization, however, is not clarified yet, and thus the evaluation by lattice dynamical analysis is expected to be useful for it.

In the present work, we show the result of the angle-resolved HREELS measurement together with the lattice dynamical analysis to understand the correlation between surface structure and the vibrational properties of the Na-adsorbed Al(111)-$(\sqrt{3}\times\sqrt{3})R30°$ structure. It should be addressed that the scheme employed here is very simple and

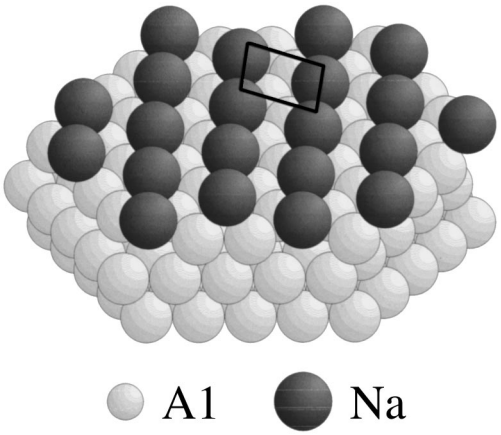

FIG. 4. ''Substitutional'' adsorption geometry of Al(111)-$(\sqrt{3}\times\sqrt{3})R30°$-Na is shown by a ''hard-ball model.'' Na atoms are located at sixfold coordinated holes of Al vacancy. A rhombus corresponds to a unit cell of the $(\sqrt{3}\times\sqrt{3})R30°$ mesh.

has a severe limitation for a precise reproduction and a very detailed analysis of the phonon structure. However, it is still expected to be useful for comparing and discussing the differences in general features of dispersion curves or their polarizations of the system with very different surface structures. In this sense, the measured phonon dispersion curves can be compared with the calculated two results based on the substitutional adsorption geometry and on a threefold adsorption geometry which can be regarded as a representative of normal adsorption geometries. Displacement vectors of the reproduced modes at the $\overline{\Gamma}$ point in each calculation are also checked whether they correspond to the measured dipole active mode at $\overline{\Gamma}$ point or not.

Figure 5 shows the measured angle-resolved HREEL spectra taken at the energy resolution of 2.3 meV (FWHM). Na coverage was monitored by a LEED observation and by a work function measurement done in the same series as the HREELS measurement. At the $\overline{\Gamma}$ point, a strong dipole active mode ($R1$) was observed at 12.5 meV, the coverage dependence of which we have reported previously.[15] As the geometry of the HREELS measurement goes off from the specular reflection, i.e., as the incident angle of the impinging electron beam decreases, the loss energy of the acoustic mode ($R2$) increases gradually and its intensity ratio to the elastic peak also becomes higher.

The plots of the loss energies versus momentum transfer $\mathbf{q}_{\parallel}$ provide the energy dispersion relations of the surface phonons. Obtained phonon dispersion curves along the $\overline{\Gamma K' M}$ symmetry of the two dimensional Brillouin zone are shown in Fig. 6. The data points based on the positions of the EELS peak maxima are indicated by the filled circles. For a comparison, the measured and calculated results of the clean Al(111) surface are also included in the same figure by open circles and the solid curves, respectively. In contrast to the case with clean Al(111), the observed acoustic modes ($R1$ and $R2$) appear in the surface-projected bulk phonon continua, which are the characteristics of surface resonant mode. Lattice dynamical analysis for such surface resonant modes is often more complicated than that of the pure surface localized modes which resides isolated from the bulk phonon bands. This is because surface resonant modes often couple

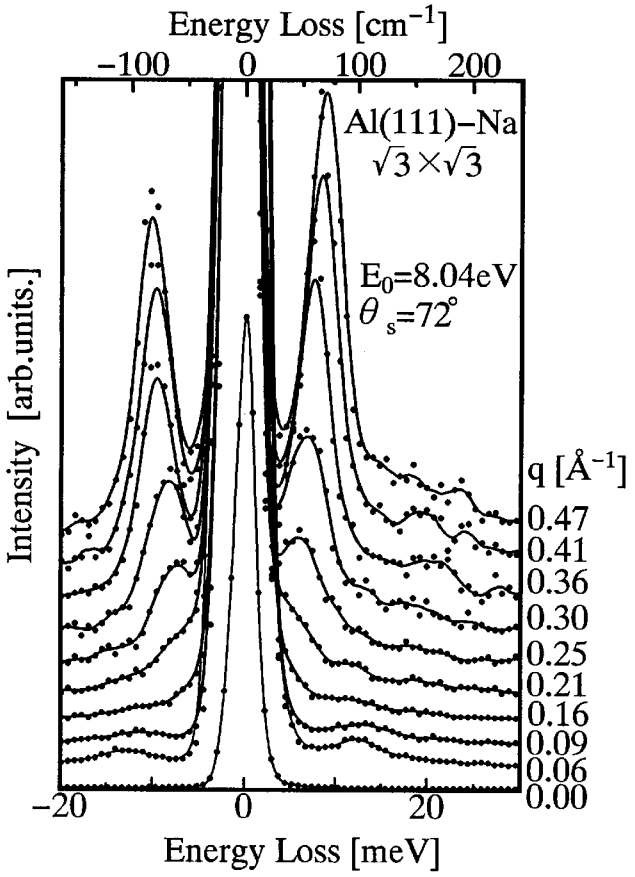

FIG. 5. A typical angle-resolved HREEL spectra of Al(111)-$(\sqrt{3}\times\sqrt{3})R30°$-Na taken at a primary energy of 8.04 eV. At around the $\overline{\Gamma}$ point, the 12.5 meV dipole active mode $R1$ is observed. When the wave vector is increased toward the $\overline{\Gamma M}$ direction, the strongly dispersing surface resonant mode $R2$ is clearly observed.

with the neighboring bulk modes, and hence the vibrational amplitude is energetically distributed over neighboring bulk modes and also spatially distributed over deeper atomic layers from the topmost layer. Where the wave vector $\mathbf{q}_{\parallel}$ is larger than 0.6 Å^{-1}, the surface localized mode $S1$ appears below the bulk accoustic phonon band.

Next, we show the calculated results for the threefold adsorption geometry. A schematics of the threefold structure is shown in Fig. 7. A slab thickness was set to 31 atomic layers as in the case with clean Al(111) to avoid the interference of the two surface phonons of which amplitude is localized at the upper and the lower surfaces. This layer thickness was evaluated to be thick enough since almost no differences have been found between the calculated phonon local density of states (LDOS) for the 31 atomic layers and that of the 121 atomic layers. The Na-adsorbed Al(111)-$(\sqrt{3}\times\sqrt{3})R30°$ structure of the threefold adsorption geometry is formed at the upper and the lower edges of this slab crystal. The spacing of the topmost Na layer and the second Al layer is set to 2.88 Å so that the Na-Al bond length is 3.31 Å, which is consistent with the results of Schmalz *et al.*[12] When we change this Na-Al bond length to the value of 3.13 Å which is derived by *ab initio* calculation by Neugebauer and Scheffler,[17] the value of phonon frequency decreases slightly (0.5 meV) at the $\overline{\Gamma}$ point which does not affect the overall

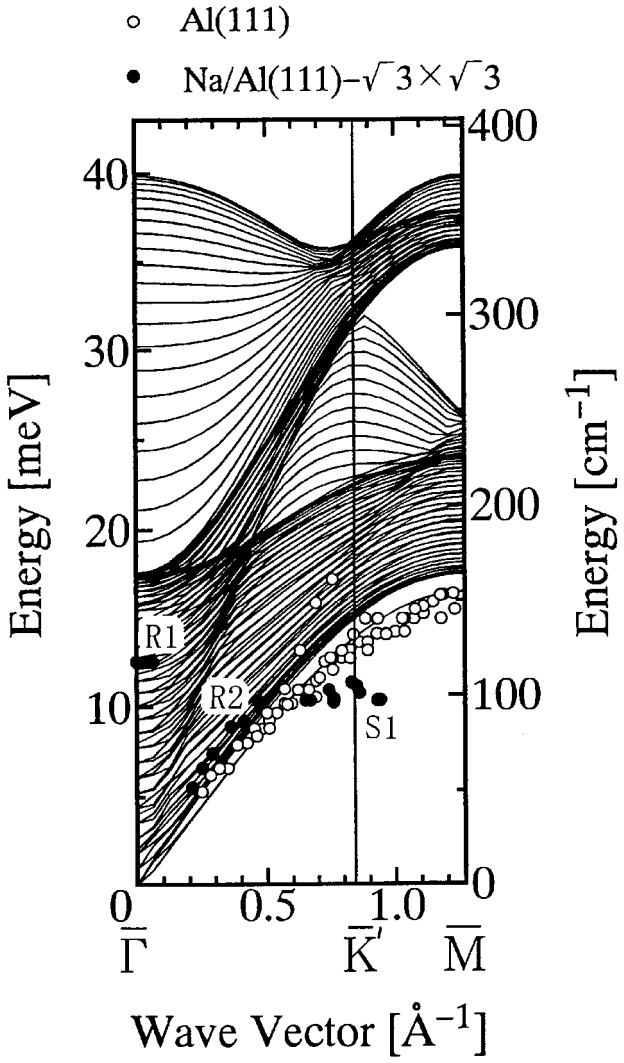

FIG. 6. The measured phonon dispersions of Al(111)-($\sqrt{3}\times\sqrt{3}$)$R30$ °-Na taken at 8.04, 16.5, 19.5 eV primary energies (filled circles). Dipole active surface resonant mode $R1$ is observed at 12.5 meV. The strongly dispersing acoustic mode $R2$ is observed above the bulk phonon edge. At around $\overline{K'}$ point, a strongly surface localized mode $S1$ appears within the bulk band gap. For a comparison, calculated and measured phonon dispersions for clean Al(111) are shown together by solid curves and open circles, respectively.

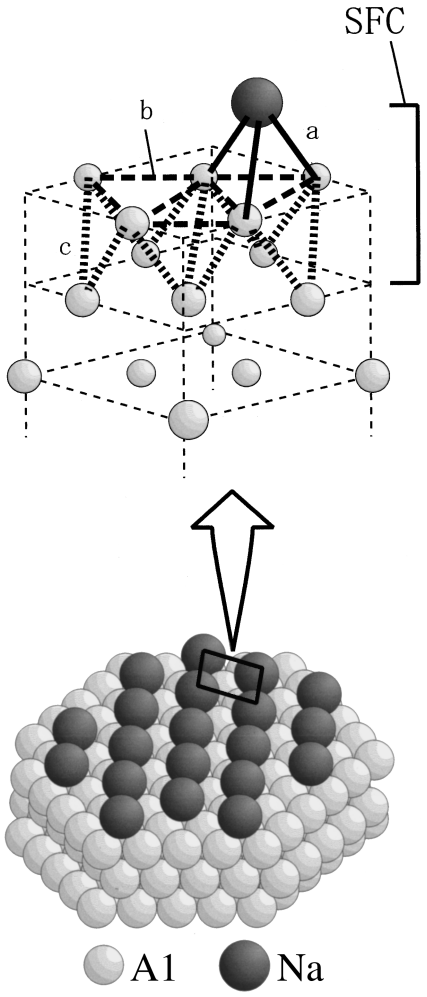

FIG. 7. Schematics of the atomic arrangement and the SFC's of a threefold adsorption geometry. The upper figure is the magnified view of a unit cell in the lower figure. Three essential SFC's (**a**, **b**, and **c**) are mainly used as fitting parameters. Other parameters up to 2NN are included in the program but set to 0 for the present discussion.

feature of the dispersion curves. BFC's of the inner part of the slab are the same as those listed in Table I. In this calculation, to make the fitting procedure simpler and assure the uniqueness of the solution, we dared to restrict the fitting parameters to three essential stretching FC's while in the program, 14 parameters up to 2NN stretching and tangential SFC's are available. These three parameters are the stretching SFC's of a 1NN Na-Al bond, a 1NN Al-Al bond in the first Al layer, and a 1NN Al-Al bond between the first and the second Al layers. All the tangential SFC's and 2NN stretching SFC's were neglected since their values are smaller than 1NN stretching SFC's by about one order of magnitude. The observed surface modes were fitted by the peak tops of the LDOS at the topmost Na layer since in the case of the resonant modes, the amplitude of these modes are blurred in their energy position and fitting by a single branch would lead to a wrong conclusion.

The calculated best fitted dispersion curves for the surface phonons are shown in Fig. 8(a). In Fig. 8(b), the phonon local density of states at the topmost Na layer at Γ point is plotted. Bold lines in Fig. 8(a) correspond to the energy positions of peak tops in LDOS's at the surface top layer at each wave vector. The surface resonant $R1'$ mode has a Na stretching motion against the substrate. Hence, its energy and displacement vector seems to be consistent with the observed dipole active $R1$ mode. In the calculation, an observed $R2$ mode is not reproduced by any combination of SFC's. Instead, the $R1'$ mode stretches over $\mathbf{q}_{\parallel}$=0.0–0.5 and the $S1'$ mode emerges within the lower phonon band gap for higher wave vectors. These two modes have displacement vectors almost perpendicular to the surface but their dispersion is rather small unlike the observed $R2$ mode. The small dispersion of $R1'$ and $S1'$ is explained in terms of the small surface parallel component of the restoring force applied to Na. The orientation of the Na-Al bond is steep like the case with adsorbed gaseous molecules on an unreconstructed sur-

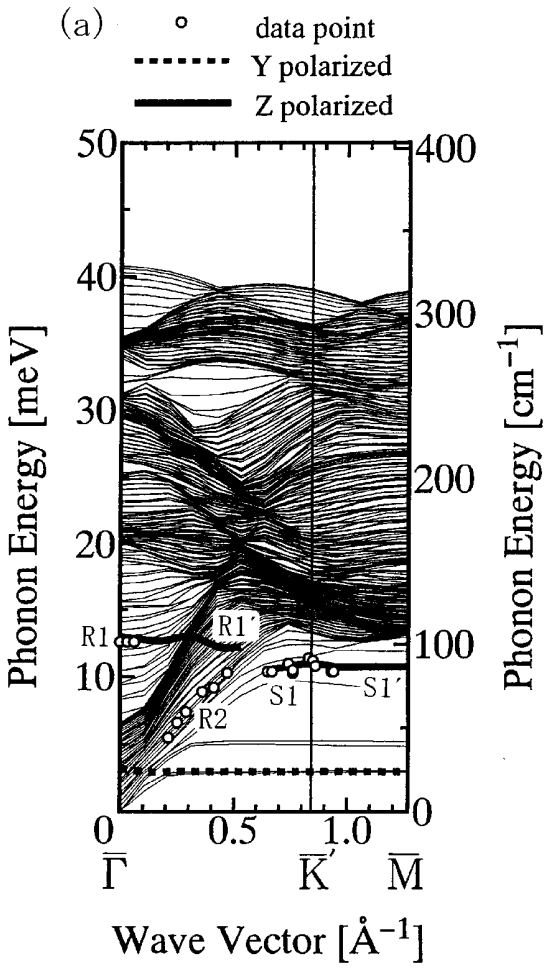

FIG. 8. (a) Calculated ($R1'$, $S1'$) and measured ($R1$, $R2$, $S1$) phonon dispersions for Al(111)-($\sqrt{3}\times\sqrt{3}$)$R30°$-Na with a threefold adsorption geometry are shown. Two z-polarized modes $R1'$ and $S1'$ (thick curves) can be fit to the experimentally observed $R1$ and $S1$ modes. However, it is impossible to reproduce the strongly dispersing $R2$ mode by this model. (b) Calculated phonon LDOS of the topmost Na ($l=1$), first Al ($l=2$), and second Al ($l=3$) at the $\bar{\Gamma}$ point are shown. The strongly z-polarized resonant mode $R1$ appears as a broad feature around 12.5 meV in the topmost LDOS ($l=1$).

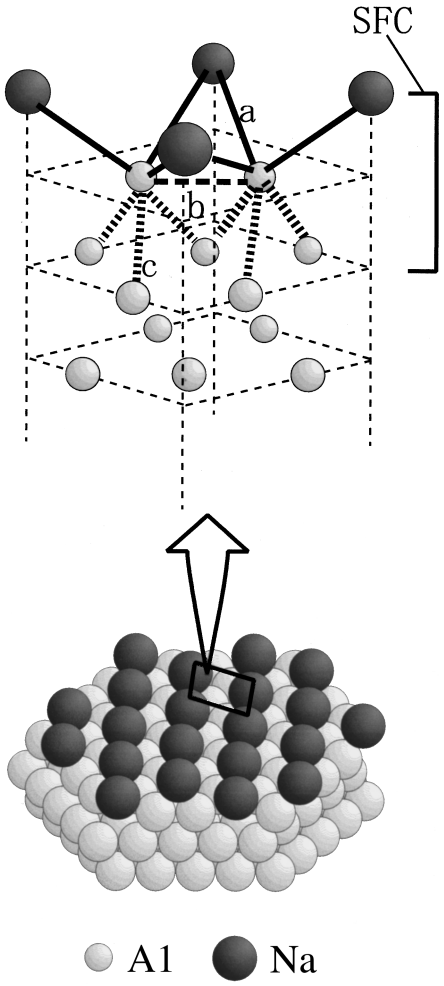

FIG. 9. Schematics of the atomic arrangement and the SFC's of a substitutional adsorption geometry. The upper figure is the magnified view of a unit cell in the lower figure. Three essential SFC's (**a**, **b**, and **c**) are used as fitting parameters. Other parameters up to 2NN are included in the program but set to 0 for the present discussion.

face and thus the restoring force parallel to the surface is small. Also, the appearance of the extremely-low-frequency longitudinal (y-polarized) surface mode is easily understood in terms of this small restoring force parallel to the surface. From the present HREELS measurement, any clear evidence of this mode was not observed.

From the discrepancies between the observed and the calculated phonon dispersions, especially from the fact that largely dispersing $R2$ mode is never reproduced by this model, we exclude the possibility of the threefold adsorption geometry. Other adsorption geometry like an on-top site or bridge site is also excluded since the orientation of their Na-Al bond is steeper than the threefold site and their phonon branches must be more dispersionless than those of threefold site.

Next, we discuss the calculated results of the substitutional adsorption geometry. Figure 9 shows the schematics of the substitutional adsorption geometry. Again, for the sake of a unique determination of the best SFC's combination, we adjusted the value of only three essential 1NN stretching FC's as fitting parameters while all the other tangential FC's

and 2NN FC's were omitted. The distance of the topmost Na layer and the first Al layer was set to the value of 1.69 Å, which is consistent with the results of Schmalz *et al.*[12] The best-fitted calculated phonon dispersion curves are shown in Fig. 10(a) and the corresponding LDOS's at $\overline{\Gamma}$ point are shown in Fig. 10(b). The determined combination of SFC's are listed in Table II together with that of the threefold geometry. Roughly speaking, the value of the 1NN Na-Al SFC is several times larger than that of the 1NN Na-Na bulk stretching FC and is almost the same magnitude as that of the 1NN Al-Al bulk stretching FC.

The calculated result based on the substitutional site is very different in two points from that of the threefold site. First, the low-frequency longitudinal mode is absent in this result. Second, the experimentally observed $R2$ mode is reproduced as well as the $R1$ and $S1$ mode. These features are clearly explained in terms of the characteristics of the substitutional adsorption geometry. Since the Na atoms are half embedded into the sixfold coordinated hole of the Al substrate, the bond angle is more slanted than the cases with other ordinary adsorption sites, e.g., threefold site. The slanted bond makes the surface parallel component of the restoring force stronger and this strengthened restoring force along the surface makes the surface longitudinal (y-polarized) mode go up into the bulk phonon band. Also, a stronger restoring force along the surface means that the interaction between the adsorbates (mediated by topmost Al atoms) is stronger and phonons are easily propagating along the surface. Thus, strongly dispersing surface mode like $R2$ is possible in contrast to the case with other ordinary adsorption geometries. Since the $R2$ mode is the same transverse acoustic mode like the Rayleigh mode, one can easily understand the resemblance between $R2$ and Rayleigh modes. Since Na is not completely embedded in the first Al layer, the surface normal component of the restoring force of the 1NN Na-Al bond is nonzero. This restoring force makes the $R2$ mode go up into the bulk phonon band in spite of the weak 2NN Na-Al forces.

The origin of the $R1$ mode is also the transverse acoustic mode since this mode is the backfold of $R2$ due to the creation of the new surface Brillouin zone of $(\sqrt{3}\times\sqrt{3})R30°$ periodicity. The atomic motion of this mode is a Na perpendicular motion against an almost fixed substrate which is consistent with the experimentally observed dipole active mode. The $S1$ mode is a strongly surface localized mode, the displacement vector of which is also similar to the Rayleigh mode of the clean surface. It should be noted that the quantitative discrepancy between the measured and the calculated $R2$ mode shows the limitation of this scheme due to the simplicity, i.e., using only three SFC's for the fitting parameters. When we increase the number of SFC's up to 2NN, the discrepancy becomes smaller, but the uniqueness of the solution is then questionable. Displacement vectors of the modes, on the other hand, are not affected so much as far as drastic changes are not applied to the 1NN SFC's. At this moment in the present work, above quantitative mismatch does not affect the essential point of the above discussions since here we only deal with the essential differences in the general feature of the phonon structure.

Comparing the above two calculated results, from the standpoint of lattice dynamics, we can say that substitutional adsorption geometry is the most possible surface structure for the Al(111)-$(\sqrt{3}\times\sqrt{3})R30°$-Na surface. According to our simple semiempirical analysis, the observed $R1$ mode is ascertained to be a strong z-polarized motion of Na atoms against the almost fixed substrate (Fig. 11) which is often assumed in some first-principles phonon calculations.[17,18] In this sense, the phonon modes dealt with in those works can be directly compared with our experimental results of 12.5 meV.

C. Phonon dispersion curves of Al(111)-(2 × 2)-Na

In this section, we show the phonon dispersion curves of the Na-adsorbed (2×2) structure which is formed after further deposition from the $(\sqrt{3}\times\sqrt{3})R30°$ structure formation. The specular HREEL spectrum shows a peak at the energy of 15 meV which is not formed by the continuous shift from the 12.5 meV peak of the $(\sqrt{3}\times\sqrt{3})R30°$ structure. This strongly indicates the reconstruction to an atomic arrangement different from that of the $(\sqrt{3}\times\sqrt{3})R30°$ structure. At the deposition time 1.5 times larger than that corresponding to the sharpest and the most intense $(\sqrt{3}\times\sqrt{3})$ LEED pattern ($\theta=1/3$), the EELS 15 meV peak intensity shows an abrupt increase which is probably due to the completion of the 2×2 structure. This deposition time corresponds to $\theta=1/2$ if the sticking probability of Na is constant throughout the deposition. This coverage is consistent with that determined by previous experiments.[26] As far as the structure model is concerned, a number of different models have been proposed.[4,27–30] Recently, however, quantitative agreements have been achieved between the results of *ab initio* total energy calculations, LEED, SEXAFS,[31,32] and XPD (Ref. 34) studies. These studies have shown that the first four layers of the structure consist of a Na-Al-Na sandwich on a reconstructed Al substrate layer.

Figure 12 shows the phonon dispersion curves for the Al(111)-(2×2)- Na surface. Filled circles are the data points of the Al(111)-(2×2)-Na and the open circles are the Rayleigh mode of the clean Al(111) surface. In spite of the large difference in the surface structure, the resemblance between the phonon dispersion curves of the two surfaces is striking. This coincidence might be more clearly seen if one transfers the upper branch $R1$ by the mirror plane placed at the $\overline{M'}$ point. From this resemblance, it is plausible that $S1$ is a transverse acoustic mode displacement vector of which is almost similar to that of the Rayleigh mode, and $R1$ might be a transverse optical mode originating from a backfold of the $S1$ mode. In the present paper, however, the lattice dynamical analysis as discussed in Sec. III B is not done for this system. This is because, in this system, a number of SFC's must be adjusted to fit to only two phonon branches and thus a unique solution is very difficult to find. However, the possibility of normal adsorption geometries can be, in this system also, excluded since the strongly dispersing modes $R1$ and $S1$ are present. The presence of these strongly dispersing modes seems to suggest a substitutional or an intermixed surface structure. The lattice dynamical calculations using SFC's determined by *ab initio* pseudopotential calculations, for example, will be the next step in analyzing the measured

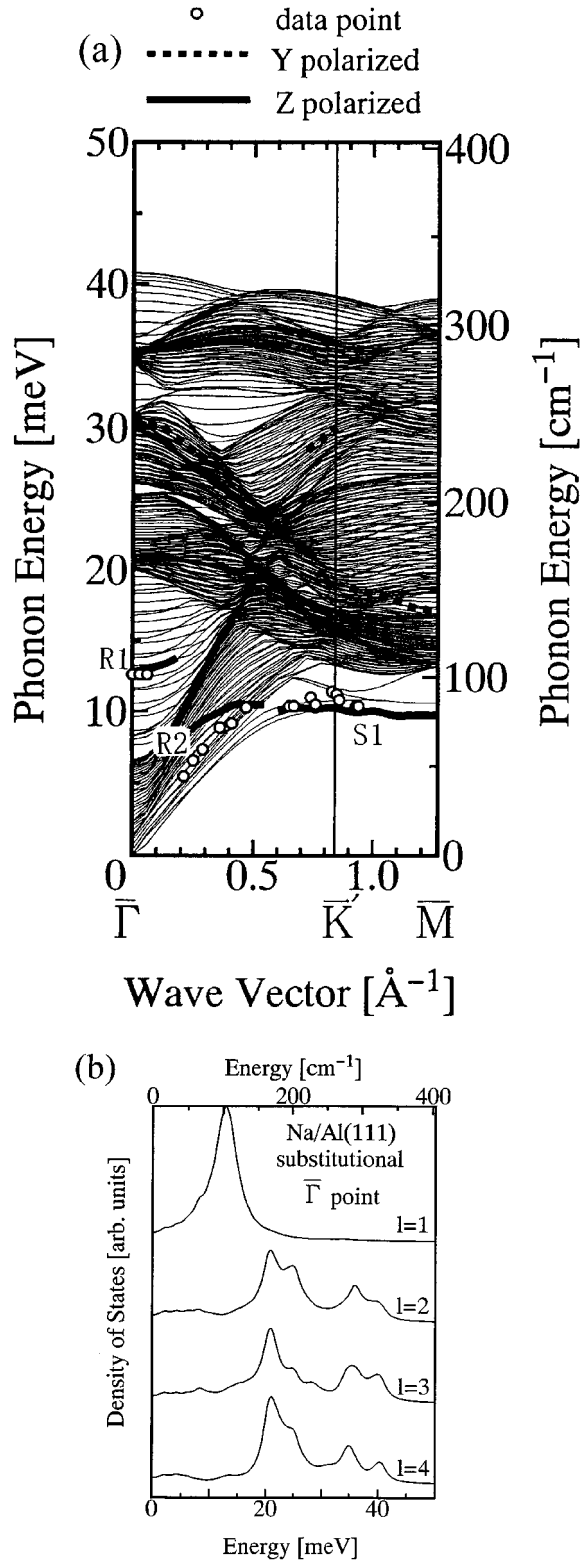

FIG. 10. (a) Calculated phonon dispersions for Al(111)-($\sqrt{3}\times\sqrt{3}$)$R30°$-Na with substitutional adsorption geometry. Three z-polarized modes $R1$, $R2$, and $S1$ were successfully reproduced by this model. Thanks to the large surface parallel component of the restoring force at Na, the strongly dispersing $R2$ mode is well reproduced by this model. (b) Calculated phonon LDOS of the topmost Na ($l=1$), first Al ($l=2$), second Al ($l=3$), and third Al ($l=4$) at the $\bar{\Gamma}$ point are shown. The strongly z-polarized resonant mode $R1$ appears as a broad feature around 12.5 meV in the topmost LDOS ($l=1$).

TABLE II. The best combinations of the FC values for the two different Al(111)-($\sqrt{3}\times\sqrt{3}$)$R30°$-Na structures. Threefold adsorption geometry (left), and substitutional adsorption geometry (right).

Bond	SFC (for threefold site) (N/m)	SFC (for substitutional site) (N/m)
a	6120	18800
b	20400	20400
c	20400	30600

phonon branches in detail and in understanding further the dynamical properties of the Al(111)-2×2-Na surface.

IV. SUMMARY

In this paper, we showed the phonon dispersion measurement for metal-induced superstructures on metal surfaces. The measured phonon dispersion curves for Na-adsorbed Al(111)-($\sqrt{3}\times\sqrt{3}$)$R30°$ were compared with that of the clean Al(111) surfaces and analyzed on the basis of a lattice dynamical calculation. The observed $S1$ mode was assigned to be a transverse surface mode. The surface resonant mode $R2$ and $R1$ was identified as an acoustic transverse mode and its backfold, respectively. The observed phonon frequency of 12.5 meV of $R1$ at the $\bar{\Gamma}$ point can be compared directly to the results from some *ab initio* calculations since $R1$ has a perpendicular motion of Na atoms against the almost fixed

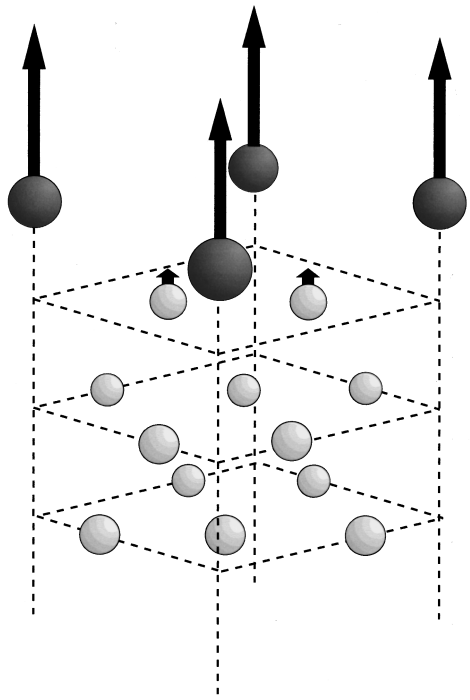

FIG. 11. Schematic view of the calculated displacement vectors of the $R1$ mode. Na atoms have large z-polarized displacement vectors while Al atoms in the second layer move only slightly. The magnitudes of the displacement vectors of the second Al atoms are less than few percent of those of the topmost Na atoms. This vibrational mode is the same mode as assumed in some *ab initio* frequency calculations.

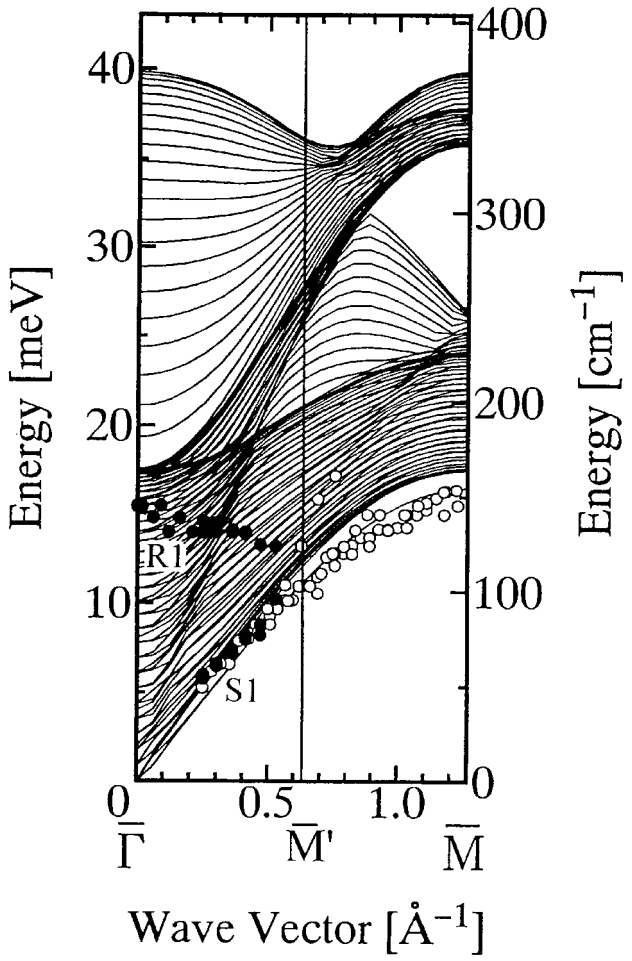

FIG. 12. Measured phonon dispersions for Al(111)-(2 ×2)-Na (filled circles) are shown. Calculated (solid curves) and measured (open circles) phonon dispersions of clean Al(111) are shown together for a comparison. The resemblance of the observed modes to the Rayleigh mode of the clean A1(111) surface is seen.

substrate. The results of the lattice dynamics showed that the substitutional adsorption geometry is the most possible one since the $R2$ mode is impossible to reproduce by other adsorption geometries. This is due to the smaller magnitude in the surface parallel component of restoring force at Na atom at normal adsorption sites. The phonon dispersion curves for the Na-adsorbed Al(111)-(2×2) surface were also measured, and found to be very close to the Rayleigh mode and its backfold of the clean Al(111) surface. The strong dispersion in the observed branches seems to exclude the possibility of normal adsorption geometry, but supports the possibility of substitutional or intermixing adsorption geometry. Finally, it should be carefully noted that the lattice dynamical analysis with the present simple model is advantageous when only the essential differences in the general feature of the phonon branches and polarization of very different surface structures are discussed. The difficulty in reproducing precisely the observed $R2$ mode may point to a limitation of the present model due to the simplicity, for example, apply-ing the central force model for the surface interatomic forces which may be noncentral due to the surface-iduced modification.[34] In this sense, the analysis using more elaborate FC models which can include the effect of surface-induced modification, models using FC's obtained from first-principles electronic structure techniques will be a next step for a more careful and detailed understanding of the present systems.

ACKNOWLEDGMENTS

The authors thank Dr. R. Souda and Dr. T. Aizawa for helpful discussions. One of the authors (T. Nagao) would like to thank Professor H. Ishida and Dr. P. Rudolf for stimulating discussions and for their close interest in this work. The lattice dynamical calculations in the present study were done using a FUJITSU VP2200 super computer under the support of the Center for Informatics Waseda University.

*Present address: Department of Physics, Faculty of Science, University of Tokyo, 7-3-1 Hongo, Bunkyo-ku, 113 Tokyo, Japan. Electronic address: nagao@phys.s.u-tokyo.ac.jp

[1] Langmuir-Gurney model: K.H. Kingdon and I. Langmuir, Phys. Rev. **21**, 21 (1923); I. Langmuir and K.H. Kingdon, Proc. R. Soc. London, Ser. A **107**, 61 (1925); J.B. Taylor and I. Langmuir, Phys. Rev. **44**, 423 (1933); R.W. Gurney, *ibid.* **47**, 479 (1935).

[2] Theoretical calculation based on Langmuir-Gurney model: J.P. Muscat and D.M. Newns, Prog. Surf. Sci. **9**, 1 (1978); N.D. Lang, in *Theory of the Inhomogeneous Electron Gas*, edited by S. Lundqvist and N.H. March (Plenum Press, New York, 1983).

[3] Experiments supporting Langmuir-Gurney model: K. Horn, A. Hohlfeld, J. Somers, Th. Linder, P. Hollins, and A.M. Bradshaw, Phys. Rev. Lett. **61**, 2488 (1988); K.-H. Frank, H.-J. Sagner, and D. Heskett, Phys. Rev. B **40**, 2767 (1989); D. Heskett, K.-H. Frank, K. Horn, E.E. Koch, H.-J. Freund, A. Baddorf, K.-D. Tsuei, and E.W. Plummer, *ibid.* **37**, 10 387 (1988).

[4] Ishida's interpretation: H. Ishida and K. Terakura, Phys. Rev. B **38**, 5752 (1988); H. Ishida, *ibid.* **38**, 8006 (1988).

[5] Experiments supporting Ishida's interpretation: P. Soukiassian, R. Riwan, J. Lecante, E. Wimmer, S.R. Chubb, and A.J. Freeman, Phys. Rev. B **31**, 4911 (1985); D.M. Riffe, G.K. Wertheim, and P.H. Citrin, Phys. Rev. Lett. **64**, 571 (1990).

[6] Enhancement of surface reactivity by alkali-metal adsorption: H.P. Bonzel, J. Vac. Sci. Technol. A **2**, 866 (1984); G. Ertl, M. Weiss, and S.B. Lee, Chem. Phys. Lett. **60**, 391 (1979).

[7] *Physics and Chemistry of Alkali Metal Adsorption*, edited by H.P. Bonzel, A.M. Bradshaw, and G. Ertl, Materials Science Monographs Vol. 57 (Elsevier, Amsterdam, 1989).

[8] K.W. Jacobsen and J.K. Norskov, Phys. Rev. Lett. **60**, 249 (1988).

[9] B.E. Hayden, K.C. Prince, P.J. Davies, G. Paoluci, and A.M. Bradshaw, Solid State Commun. **48**, 325 (1983).

[10] S.M. Francis and N.V. Richardson, Surf. Sci. **152/153**, 63 (1985).

[11] W.C. Fan and A. Ignatiev, Phys. Rev. B **38**, 366 (1988).

[12] A. Schmalz, S. Aminpirooz, L. Becker, J. Haase, J. Neugebauer, M. Scheffler, D.R. Batchelor, D.L. Adams, and E. Bøgh, Phys. Rev. Lett. **67**, 2163 (1991).
[13] J. Burchhardt, M.M. Nielsen, D.L. Adams, E. Lundgren, and J.N. Andersen, Phys. Rev. B **50**, 4718 (1994); C. Stampfl, M. Scheffler, H. Over, J. Burchhardt, M. Nielsen, D.L. Adams, and W. Moritz, Phys. Rev. Lett. **69**, 1532 (1992).
[14] M. Kerkar, D. Fisher, D.P. Woodruff, R.G. Jones, R.D. Diehl, and B. Cowie, Phys. Rev. Lett. **68**, 3204 (1992).
[15] T. Nagao, Y. Iizuka, M. Umeuchi, T. Shimazaki, and C. Oshima, Surf. Sci. **329**, 269 (1995).
[16] J.N. Andersen, M. Qvarford, R. Nyholm, J.F. van Acker, and E. Lundgren, Phys. Rev. Lett. **68**, 94 (1992).
[17] J. Neugebauer and M. Scheffler, Phys. Rev. B **46**, 16 067 (1992); Phys. Rev. Lett. **71**, 577 (1993).
[18] H. Ishida and Y. Morikawa, Surf. Sci. **291**, 87 (1993).
[19] S.A. Lindgren, C. Svensson, and L. Walldén, Phys. Rev. B **42**, 1467 (1990).
[20] P. Rudolf, C. Astaldi, and S. Modesti, Phys. Rev. B **42**, 1856 (1990); P. Rudolf, C. Astaldi, G. Cautero, and S. Modesti, Surf. Sci. **251**, 127 (1990).
[21] T. Nagao, Y. Iizuka, M. Umeuchi, T. Shimazaki, M. Nakajima, and C. Oshima, Rev. Sci. Instrum. **65**, 515 (1994).
[22] R. Stedman and G. Nilsson, Phys. Rev. **145**, 492 (1966).
[23] A. Lock, J.P. Toennies, Ch. Wool, V. Bortolani, A. Franchini, and G. Santoro, Phys. Rev. B **37**, 7087 (1988).
[24] A. Franchini, V. Bortolani, G. Santoro, V. Celli, A.G. Eguiluz, J.A. Gasper, M. Gester, A. Lock, and J.P. Toennies, Phys. Rev. B **47**, 4691 (1993).
[25] *Surface Phonons*, edited by by W. Kress and F.W. de Wette, Springer Series in Surface Sciences Vol. 21 (Springer-Verlag, Berlin, 1991), see Fig. 8.55, p. 258.
[26] K.-D. Tsuei, D. Heskett, A.P. Baddorf, and E.W. Plummer, J. Vac. Sci. Technol. A **9**, 1761 (1991).
[27] J.O. Porteus, Surf. Sci. **41**, 515 (1974).
[28] A. Hohlfeld and K. Horn, Surf. Sci. **211**, 844 (1989).
[29] M. Kerkar, D. Fisher, D.P. Woodruff, R.G. Jones, R.D. Diehl, and B. Cowie, Surf. Sci. **278**, 246 (1992).
[30] H. Brune, J. Wintterlin, R.J. Behm, and G. Ertl, Phys. Rev. B **51**, 13 592 (1995).
[31] C. Stampfl and M. Scheffler, Surf. Sci. **319**, L23 (1994).
[32] J. Burchhardt, M.M. Nielsen, D.L. Adams, E. Lundgren, J.N. Andersen, C. Stampfl, M. Scheffler, A. Schmalz, S. Aminpirooz, and J. Haase, Phys. Rev. Lett. **74**, 1617 (1995).
[33] R. Fasel, P. Aebi, L. Schlapbach, and J. Osterwalder, Phys. Rev. B **52**, R2313 (1995).
[34] *Electronic Screening in Metals: from Phonons to Plasmons*, edited by by G.K. Horton and A.A. Maradudin, Dynamical Properties of Solids Vol. 7 (Elsevier, Amsterdam, 1990).